

The Young Starburst Nucleus of the Wolf-Rayet LINER Galaxy NGC 6764

E. Schinnerer

Astronomy Department, California Institute of Technology, MS 105-24, Pasadena, CA 91101, USA

es@astro.caltech.edu

A. Eckart

Universität zu Köln, I.Physikalisches Institut, Zùlpicherstraße 77, 50937 Köln, Germany

and

Th. Boller

MPI für Extraterrestrische Physik, 85740 Garching, Germany

ABSTRACT

Near-infrared K band imaging spectroscopy of the central $8''$ (1.3 kpc) in the Wolf-Rayet LINER galaxy NGC 6764 shows that the most recent star formation is most likely still unresolved at sub-arcsecond resolution (< 100 pc). The K band continuum source has a size of about $1.5''$ (240 pc). In addition to stellar CO and Na absorption lines as well as recombination lines of H and He, the K band spectrum shows several strong emission lines from molecular hydrogen (H_2). The H_2 line emission is spatially and spectrally resolved showing a rotating ring/disk of $\sim 1.2''$ (200 pc) diameter.

An analysis of the nuclear ($3'' \sim 480$ pc) stellar light using population synthesis models in conjunction with NIR spectral synthesis models suggests following star formation history: Two starbursts with decay times of 3 Myr occurred 3 to 5 Myr and 15 to about 50 Myr ago. Continuous star formation with a SFR of $\sim 0.3 M_{\odot} \text{yr}^{-1}$ over at least 1 Gyr can also explain the observed parameter. However, the mass relocation and consumption involved as well as the different spatial distribution of the lines associated with the star formation strongly favor the 'two starburst' scenario. In that scenario, up to 35% of the total observed Br γ flux could still be due to the AGN, depending on the assumed age of the older starburst event. In contrast to other starburst galaxies (e.g. M82, NGC 7552), the younger starburst in NGC 6764 is very likely located closer to the nucleus and surrounded by the older starburst. One possible explanation can be that the stellar bar still transports gas down to radii close to the nucleus. This suggests that the massive star formation activity is directly competing with the AGN for the fuel.

We also present the results of a 44 ksec. HRI ROSAT exposure. The HRI data show

the presence of a X-ray source (probably an AGN) which varies by more than a factor of 2 over a time scale of 7 days. This implies the presence of a compact source with a discrete or at most 1000 AU source size. In addition, we find an extended X-ray component which looks similar to the radio continuum emission presented in published VLA maps. Both data sets confirm the composite nature of the center of NGC 6764: the presence of a compact AGN as well as recent violent nuclear star formation.

Subject headings: galaxies:active - galaxies:individual(NGC 6764) - galaxies:nuclei - galaxies:starburst

1. INTRODUCTION

In Wolf-Rayet (WR) galaxies the presence of the broad HeII λ 4686 feature (WR feature) signals very recent massive star formation (Armus, Heckman & Miley 1988; Conti 1991). WR galaxies therefore offer the unique possibility to study high mass star formation (Maeder & Conti 1994), since the progenitors of WR stars have initial masses $> 20 M_{\odot}$ and the WR stars themselves are younger than 10 Myr. However, it is often unclear whether the WR line emission is originating from a single isolated HII region or is associated with the nucleus of the parent galaxy itself. So far, 139 objects are listed in the new Wolf-Rayet (WR) galaxies catalog (Schaerer, Contini & Pindao 1999), as Wolf-Rayet emission features are rarely observed in galaxies. The study of WR galaxies is therefore essential for understanding the starburst phenomenon in galaxies, as it offers the unique opportunity to analyze the stellar population at a well-defined evolutionary stage.

NGC 6764 is a nearby (32 Mpc for $H_0=75$ km s $^{-1}$; $1''=160$ pc) S-shaped barred spiral galaxy (SBb), classified as a LINER galaxy based on optical spectroscopy (Osterbrock & Cohen 1982). NGC 6764 is unusual because it also displays a prominent 466 nm Wolf-Rayet emission feature at the nucleus (Osterbrock and Cohen 1982) and was already in the first WR catalog of Conti (1991). The galaxy contains a nuclear stellar optical continuum with a "width" of $\sim 1.6''$ or about 260 pc (Rubin, Thonnard, & Ford 1975).

Eckart et al. (1991) presented single dish measurements of the J=1-0 and J=2-1 rotational transitions of ^{12}CO and ^{13}CO obtained with the IRAM 30m telescope, as well as the first *JHK* images of NGC 6764. Eckart et al. (1996) presented X-ray observations, high resolution optical, millimeter-wave interferometer measurements of the 115 GHz $^{12}\text{CO}(1-0)$ line emission, the first imaging observations of the 2.12 μm H $_2$ emission, and measurements of the 2.06 μm He I and the 2.17 μm Br γ line emission toward the nucleus of NGC 6764. Their NIR and optical spectroscopic data which include the 466 nm Wolf-Rayet feature revealed a dense concentration of molecular gas in the center and a very recent (few 10^7 yr) starburst at the nucleus of NGC 6764. This starburst is most likely responsible for the presence of a few thousand Wolf-Rayet stars in the nucleus of NGC 6764 (Eckart et al. 1996).

In this paper we present the first *K* band integral field spectroscopy and ROSAT X-ray obser-

vations using the high-resolution imager (HRI) of the nucleus of NGC 6764. We describe our observations in §2, and present an analysis of the X-ray data in §3. In §4 we discuss the result from the integral field spectroscopy, and in §5 we analyze the nuclear star formation history of NGC 6764. We present a brief summary in §6.

2. OBSERVATIONS

2.1. *K* band integral field spectroscopy

NGC 6764 was observed in the *K* band ($2.2 \mu\text{m}$) on 1997, July 26 and 28 with the MPE integral field spectrograph 3D (Weitzel et al. 1996) combined with the tip-tilt corrector ROGUE (Thatte et al. 1995) at the 3.5 m telescope in Calar Alto, Spain. The image scale was $0.5''/\text{pixel}$. The total integration time on source was 2880 s. Two fields off-set by $1.5''$ in east-west direction were combined to cover the nuclear region. Since the seeing was different in both nights ($\leq 1''$ on July 26 and $\sim 1.2''$ on July 28), the data set from July 26 was convolved to the resolution of the second night for the combined data cube with a larger field of view.

3D obtains simultaneous spectra for each pixel ($R \equiv \lambda/\Delta\lambda \approx 750$ for *K* band) of an $8'' \times 8''$ field. This is done using an image slicer which rearranges the two-dimensional focal plane onto a long slit of a grism. The dispersed spectra were then detected on a NICMOS 3 array. A detailed description of the instrument and the data reduction is given in Weitzel et al. (1996). The data reduction procedure converts each two dimensional image into a three dimensional data cube with two spatial and one spectral axes. The data cubes were co-added and centered on the continuum peak. All images were dark-current and sky-background subtracted, corrected for dead and hot pixels, and spatially and spectrally flat-fielded. To correct for the effects of the Earth's atmosphere on the *K* band spectrum, a standard star was observed. This standard spectrum was first divided by a template spectrum of the same spectral type (Kleinmann & Hall 1986) in order to remove stellar features. The effect due to different zenith distance of the source and the standard star was minimized using the ATRAN atmospheric model (Lord 1992), mainly to correct for the different atmospheric absorption. The source data were then divided by the atmospheric transmission spectrum.

We flux calibrated the data adopting the integrated *K* band flux density value given by Rieke (1978) in a $8.5''$ aperture centered on the nucleus. Due to the different spatial resolution and S/N each data cube was flux calibrated individually before combination. A comparison to the line fluxes of Eckart et al. (1996) in a $5''$ aperture showed good agreement within the errors for the HeI $\lambda 2.06\mu\text{m}$ and H₂S(1) $\lambda 2.12\mu\text{m}$ lines. For Br γ $\lambda 2.16\mu\text{m}$ the obtained flux was by a factor of 2 higher. This is probably related to the fact that the Br γ line has a weak broad component (FWZI ~ 2100 km/s).

2.2. ROSAT HRI observations

NGC 6764 was observed using the HRI detector (David et al. 1996) on board the ROSAT satellite (Trümper 1983) between 1995 September 2 (10:23:45 UT) and 1995 September 19 (10:23:38 UT). The total exposure time was 44660 s and the source was centered on-axis in the field of view. The centroid position of NGC 6764 in the HRI image, computed from a Gaussian fit to the spatial distribution is $\alpha_{2000} = 19^h08^m16.^s22 \pm 0.03s$, $\delta_{2000} = +50^{\circ}56'2.20'' \pm 0.59''$. The internal ROSAT HRI pointing error is of the order of $\pm 5''$. The source cell size was obtained from a radial profile of counts within a ring centered on the centroid position of NGC 6764. For distances larger than $25''$ from the centroid position the radial profile is consistent with the background level. The number of source plus background photons within a radius of $25''$ is 457 ± 21 . The background was determined in a ring around the source with an inner radius of $40''$ and an outer radius of $80''$. The number of background photons normalized to the source cell size is 109 ± 10 . The resulting number of source photons is therefore 348 ± 25 corresponding to a mean count rate of $(7.8 \pm 0.3) \times 10^{-3} \text{ counts s}^{-1}$.

3. ROSAT HRI RESULTS

Our HRI data show both the presence of an X-ray source that strongly varies on the time scale of several days and an additional extended X-ray component that looks similar to published VLA radio continuum maps. Both findings confirm the composite nature of the center of NGC 6764: The presence of a compact active nucleus and recent nuclear star formation (see also Gonçalves, Veron-Cetty & Veron 1999).

3.1. X-ray Variability

For the extragalactic sources studied by Walter & Fink (1993) with the ROSAT PSPC the weighted mean photon index is 2.3 with an uncertainty of 0.03. Due to the limited photon statistics the PSPC observations of the ROSAT All-Sky Survey of NGC 6764 do not constrain the spectral X-ray properties. Therefore, we have used the spectral shape of a simple power-law model with an photon index Γ of 2.3 and an absorbing column equal the Galactic absorption by neutral hydrogen of $6.0 \times 10^{20} \text{ cm}^{-2}$ towards NGC 6764 (Dickey & Lockman 1990). We derive that the mean HRI count rate of $7.8 \times 10^{-3} \text{ counts s}^{-1}$ corresponds to an absorption-corrected 0.1-2.4 keV flux of $7.13 \times 10^{-13} \text{ erg cm}^{-2} \text{ s}^{-1}$ (see Fig. 1). Using equation (7) of Schmidt & Green (1986) (with $H_0 = 75 \text{ km s}^{-1} \text{ Mpc}^{-1}$ and $q_0 = \frac{1}{2}$) we find that the mean HRI count rate of NGC 6764 corresponds to an isotropic luminosity of $8.71 \times 10^{40} \text{ erg s}^{-1}$ or about $2.3 \times 10^7 L_{\odot}$ fully consistent with the luminosity derived by Eckart et al. (1996). Here we assume that the radiation is isotropically radiated and that relativistic beaming effects are not relevant for the derived value of the luminosity. Kriss, Canizares & Ricker (1980) give an upper limit of the X-ray flux of NGC 6764 of $L_X < 8.6 \times 10^{40} \text{ ergs s}^{-1}$ over the (0.5 – 4.5 keV) energy band.

An examination of the arrival times of the X-ray photons shows deviations from the mean count rate and suggests the presence of variability on very short time scales. Fig. 1 displays the ROSAT HRI light curve obtained for NGC 6764 between 1995 September 2 and 19. The exposure times for the individual data points range between 1575 seconds (Offset Julian date 7.9) and 26520 seconds (Offset Julian date 0.0). The integration time per bin is always larger than 1550 seconds to avoid apparent count rate variations due to the ROSAT wobble. NGC 6764 shows count rate variations by a factor of about 2 on a time scale of 7 days. A constant light curve model can be rejected with 97.6 per cent confidence based on a χ^2 statistic. The continuous decrease of the ROSAT HRI count rate starting at day 7.9 of the observations further accounts for true changes of the X-ray emission in the distant Wolf-Rayet LINER galaxy NGC 6764. The presence of an extended X-ray component (discussed in section 3.2) that accounts for about half of the total luminosity suggests that the observed variability (if entirely attributed to a nuclear source) was significantly higher than a factor of 2.

The minimum count rate of 5.95×10^{-3} counts s^{-1} was observed at day 1.5 within a 4760 second exposure time interval. The maximum count rate is 1.34×10^{-2} counts s^{-1} observed at day 7.9 within a 1575 s exposure interval. The light curve of NGC 6764 shows a continuous decline of the count rate starting at day 7.9 up to the end of the observations. Such count rate variations suggest that a major fraction of the variable X-ray emission originates close to a super-massive black hole. Assuming that the variability is not affected by beaming or relativistic motions the upper limit for the size of the variable X-ray emission is $R \approx \Delta t c \approx 1.6 \times 10^{16}$ cm or only about 10^3 AU.

3.2. Extended X-ray emission

The X-ray emission originating from NGC 6764 shows a complex structure: In addition to a source component (see Fig. 2) at the nuclear position, we find an extended structure with indications for different centers of enhanced X-ray emission north-west and south-west of the central position. The extended emission accounts for about half of the total X-ray luminosity in the 0.1-2.4 keV band derived from the mean count rate. If parts of the extended emission are due to a soft X-ray spectrum, this suggests that the X-ray luminosity of this extended component is either due to Bremsstrahlung emission or an emission line dominated spectrum. With the ROSAT HRI and also the PSPC observations we are not able to differentiate between Bremsstrahlung models and an emission line dominated spectrum from hot diffuse gas based on the model calculations of Raymond & Smith (1977). The derived plasma temperatures of both models are consistent within the errors. This would be in agreement with emission from a very diffuse component in addition to a contribution from compact sources indicated by our data and expected from supernovae, hot stars, and X-ray binaries. Eckart et al. (1996) have shown that the X-ray luminosity could be entirely explained by the energy input of supernovae, and that the total mass of hot gas probably amounts to several $10^6 M_{\odot}$.

Starburst galaxies show typical values of 10^{-2} to 10^{-4} for their L_X/L_{FIR} ratios (Boller 1999). The L_X/L_{FIR} ratio for NGC 6764 lies within the range expected for starburst, if we use the X-ray luminosity for the extended component of $L_X \sim 1.15 \times 10^7 L_\odot$ and a total far-infrared luminosity of $L_{FIR} \sim 2 \times 10^{10} L_\odot$. As discussed in section 5.1 about 40% of the far-infrared luminosity can be attributed to the nuclear starburst (inner ~ 250 pc). This leaves still enough luminosity for the extended component. Therefore, we find that the L_X/L_{FIR} ratio of the extended X-ray emission in NGC 6764 is in agreement with those found for starburst galaxies. The spatial extent of the extended emission of $\sim 10''$ FWHM (~ 1.6 kpc) is similar to the extent of starburst rings of about 1 to 2 kpc.

We also note that the extended X-ray structure is similar to the structure found in the VLA radio maps (Ulvestad, Wilson, & Sramek 1981; Wilson & Willis 1980). Baum et al. (1993) discussed the origin of the radio emission suggesting strong star formation and due to the alignment of the radio emission with the minor kinematic axis pressure driven outflow. A large-scale $H\alpha$ map shows extended nuclear $H\alpha$ emission over the inner $10''$ (D. Frayer, private communication). This suggests that the hot X-ray emitting gas and the synchrotron radiation emitting relativistic gas component are spatially coexisting and probably both are a result of strong recent circum-nuclear star formation.

4. K BAND INTEGRAL FIELD SPECTROSCOPY RESULTS

The nuclear K band spectrum is dominated by emission lines from warm molecular H_2 . The slope of the continuum indicates no strong dilution from non-stellar sources like dust emission or AGN power law contribution. The K band continuum map gives a source size of about FWHM $2.2'' \times 1.7''$ (PA $\sim 95^\circ$), larger than the seeing of $1.2''$. This implies that the K band continuum source is extended with an intrinsic source size of about $1.7'' \times 1.2''$ (PA $\sim 95^\circ$). This is quite consistent with the July 26 data, where we obtained an uncorrected source FWHM of $1.8'' \times 1.3''$ (PA $\sim 95^\circ$).

We made line maps for all the lines indicated in Fig. 3 by averaging the adjacent continuum channels and subtracting the resulting mean from all channels. These line channels were subsequently co-added. All fluxes and equivalent widths (EWs) are measured in circular apertures, the corresponding errors are the standard deviations (1σ) for the given apertures in the line maps (Tab. 1 and 2) and do not include calibration uncertainties or systematic effects which we estimate to be of the order of 10%. All calculations for the stellar population synthesis are made for a $3''$ (480 pc) aperture.

4.1. The H and He Recombination Lines

The $Br\delta$, $Br\gamma$ and HeI line emission is spatially unresolved at our resolution. The comparison of the FWHM in the line maps and the adjacent continuum channels shows clearly that the extent

of the emission lines is more compact than the continuum emission (Fig. 4). This indicates that the line emission is arising in a region considerably smaller than 150 pc (about 1"). The ratio of $\text{Br}\delta/\text{Br}\gamma \sim (0.61 \pm 0.12)$ is consistent with values of 0.65-0.67 expected for 'case B recombination' (Osterbrock 1989) which suggests that extinction only plays a minor role at these wavelengths (see also Eckart et al. 1996).

Assuming that the HeI 2.06 μm and $\text{Br}\gamma$ line emission is arising in HII regions around hot, young stars, the HeI/ $\text{Br}\gamma$ ratio can be used to estimate the mean effective temperature T_{eff} of these ionizing stars. We observe a ratio of 0.46 ± 0.04 indicating $T_{eff} \sim 35\,000$ K, representative of an O8 star dominated ionizing stellar population. Note that we neglected effects like mixed-in dust and differences in the velocity structure of the Strömgren spheres (see Lançon & Rocca-Volmerage 1996, Doherty et al. 1995). Since NGC 6764 is classified as a LINER, we could expect some AGN contribution to the $\text{Br}\gamma$ line emission, making the effective temperature a lower limit (see also section 5.3.1). This is consistent with the finding that about 66% (72%) of the nuclear $\text{H}\alpha$ ($\text{H}\beta$) line emission which is coming from a narrow line component is of stellar origin (i.e. consistent with HII region line ratios; Gonçalves, Veron-Cetty & Veron 1999).

4.2. The H₂ Emission Lines

The H₂1-0 S(1) line is the strongest of all the six H₂ lines detected with a $\text{S/N} \geq 3$ in the *K* band spectrum. The H₂1-0 S(1) emission is extended in the east-west direction with a FWHM of $\sim 3.3''$ (500 pc corrected for seeing) in the line maps (see also Eckart et al. 1996). The extent is even larger than that in the *K* band continuum of $2.2''$. The maximum of the line emission is off-set by about $0.25''$ east from the continuum peak. The H₂1-0 S(1) line has a FWZI of ~ 950 km/s. Line maps of the blue and red line wing (centered ± 270 km/s of the line center with widths of 400 km/s) show a shift in the emission distribution from the south-west to the north-east indicating a rotating gas disk or ring. The emission peaks of the blue and red line wings are about $1.2''$ (200 pc) apart. These observed kinematics and distribution of the warm molecular gas are similar to those of the cold molecular gas observed in its ¹²CO line emission (Schinnerer et al. in prep.).

4.3. The Stellar Absorption Lines

The CO absorption band heads at $\lambda 2.29 \mu\text{m}$ are clearly visible in the spectrum (Fig. 3). In addition the NaI absorption at $\lambda 2.21 \mu\text{m}$ is most likely detected, all those lines indicate the presence of cool, evolved stars. The spatial extent of the stellar absorption lines coincides with the extent of the *K* band continuum (Fig. 4), in contrast to the H and He recombination lines which are spatially unresolved at our resolution. The situation therefore indicates that the hot, young stars and the cool, evolved stars are distributed differently.

Using the measured equivalent widths (EWs) of the detected stellar absorption features and their

ratios, it is possible to classify the mean stellar type (e.g., Origlia, Moorwood & Oliva 1993, Oliva et al. 1995, Förster-Schreiber 2000). The ^{12}CO 2-0/NaI ratio of (4.57 ± 1.56) is consistent with effective temperatures T_{eff} between 3000 K and 4800 K. The $^{12}\text{CO}(2-0)/^{13}\text{CO}(2-0)$ ratio indicates a $T_{eff} \leq 4500$ K, since these lines are vanishing for effective temperatures > 4500 K (Förster-Schreiber 2000). Assuming that the total K band continuum is due to cool stars and that the measured equivalent widths (Table 2) are not diluted, a comparison to EW of standard stars (e.g. Origlia, Moorwood, Oliva 1993, Schreiber 1998) suggests the presence of either late K supergiants or early M giants. Under the assumption that there is a continuum flux density contribution from younger stars (indicated by the HeI and Brackett emission) and from the AGN, the mean stellar type has to be even cooler since in this case the CO band heads appear diluted and are therefore deeper than actually measured. The cool, evolved stars can be either members of a few Myr old starburst (being mostly red supergiants, RSGs) or part of an older stellar population (being mostly red giants, RGs).

5. THE NUCLEAR STAR FORMATION HISTORY

To investigate the nuclear star formation history further, we use the population synthesis code STARS (Sternberg & Kovo, private communication) which was successfully applied to a number of galaxies (NGC 1808: Krabbe, Sternberg & Genzel 1994, NGC 7469: Genzel et al. 1995, NGC 7552: Schinnerer et al. 1997, IC 342: Böker et al. 1997, Circinus: Maiolino et al. 1998, M 82: Schreiber 1998, NGC 3227: Schinnerer et al. 2000) in conjunction with the NIR spectral synthesis code SPECSYN (Schinnerer et al. 1997, 2000).

The model is similar to other stellar population synthesis models (e.g. Lançon & Rocca-Volmerange 1996, Leitherer et al. 1999) and includes the most recent stellar evolutionary tracks (Schaerer et al. 1993, Meynet et al. 1994). A summary of the systematic uncertainties in the population synthesis models is given in Leitherer et al. (1999); for a discussion of the AGB phase which is implemented in STARS see Oliva & Origlia (2000). STARS gives output observable parameters such as the bolometric luminosity L_{bol} , the K band luminosity L_K , the Lyman continuum luminosity L_{LyC} , and the supernova rate ν_{SN} , as well as the diagnostic ratios between these quantities: L_{bol}/L_{LyC} , L_K/L_{LyC} and $10^9 \nu_{SN}/L_{LyC}$. All three ratios are measures of the time evolution and the shape of the IMF, with slightly different dependencies on the exponential slope α and the upper mass cut-off m_u . Hertzsprung-Russell diagrams (HRDs) representing the distribution of these luminosities are calculated. SPECSYN uses the distribution of the K band luminosity L_K within a HRD (from STARS) to weight standard star spectra of different spectral type and luminosity (Schinnerer et al. 1997, 2000). In addition, effects like extinction or non-stellar contributions from dust emission or an AGN can be included as well.

5.1. The Parameters for the Population Synthesis

To estimate L_{bol} for the central 3" (~ 500 pc) of NGC 6764 we followed the approach of Eckart et al. (1996). For starburst regions the FIR luminosity can be assumed to be equivalent to the bolometric luminosity (Telesco, Dressel & Wolstencroft 1993). Under the assumption that the relative contribution from the star forming regions is similar at all the IRAS wavelengths, we scaled the IRAS fluxes by 0.4 at 12 μm (0.36 Jy), 25 μm (1.29 Jy), 60 μm (6.33 Jy) and 100 μm (11.56 Jy) accordingly to the measured 10.6 μm flux in a 5" aperture (Rieke 1978). Since the 10.6 μm measurement of Rieke (1978) and the IRAS 12 μm measurement have similar filter width of ~ 5 μm and the strong absorption and emission features in the mid-IR spectrum of NGC 6764 (Rigopoulou et al. 1999) are covered in both measurements, this approach seems justified to obtain the nuclear mid- and far-IR emission. To derive L_{bol} the relation given by Sanders & Mirabel (1996) was used. This approach was examined in the case of NGC 7552, there similar values for L_{bol} were obtained by using different methods (Schinnerer et al. 1997).

L_K and L_{LyC} were estimated via the equations given in Genzel et al. (1995) (using a $\delta\lambda = 0.6\mu\text{m}$ as the K band width) and taking the values measured with 3D in a 3" aperture. For ν_{SN} we used the empirical relation between the 5 GHz flux and ν_{SN} given by Condon (1992). To derive the actual value, we only used the nuclear 5 GHz flux of 3.4 mJy from Baum et al. (1993), since the H/He recombination lines as well as the stellar absorption lines are smaller in extent than the nuclear radio source size. The derived quantities are listed in Tab. 3. (All equation are described in Schinnerer, Eckart, & Tacconi 1998.)

5.2. Evidence from Wolf-Rayet features

Eckart et al. (1996) found that the WR feature at 4660 \AA (NIII $\lambda 4640$ and HeII $\lambda 4686$) is spatially extended. However, the 3D HeI and Br γ line maps show no indication for extended emission which may be due to our sensitivity. The optical line emission is mainly due to N-rich WR stars (subtype WN) (Eckart et al. 1996). In their recent optical data Kunth & Conti (1999) were able to identify a WR feature at CIII $\lambda 5696$ and CIV $\lambda 5808$ arising from C-rich WR stars (subtype WC).

In the K band, the C IV and C III lines at 2.08 μm and 2.11 μm , respectively, are expected from WC stars (Figer, McLean, & Najarro 1997) which are not detected in the 3D data at our sensitivity. We see indication for the HeI/HeII line complex at 2.16 μm (Fig. 3 and 5) indicative of the presence of WN stars (Figer, McLean, & Najarro 1997). Since in late WN stars this line complex is almost as prominent as the 2.06 μm HeI line (Figer, McLean, & Najarro 1997), this implies that most of the line emission seen at 2.06 μm is due to HII regions and not WR stars.

Population synthesis results of WR populations show that considerable numbers of WN stars (in addition to WC stars) are present after about 3 Myrs (Schaerer & Vacca 1998). At about 5 Myrs WN stars clearly dominate the WR star population and the strength of the C IV $\lambda 5808$ line (indicating WC stars) decreases whereas the WR features at $\lambda 4660\text{\AA}$ (indicating WN stars) start to increase

significantly. The presences of both WN and WC stars therefore suggests an age between 3 and 5 Myrs for the nuclear stellar population in NGC 6764 associated with the WR stars.

5.3. Modeling: General Remarks

In our starburst model calculations, we used a Salpeter IMF with a lower mass cut-off of $1 M_{\odot}$ and an upper mass cut-off of $120 M_{\odot}$. The WR stars signal that massive star formation has occurred recently or is still ongoing. On the other hand, an older stellar population that produces most of the K band continuum must be present. Therefore only two simple scenarios can be considered producing the observed properties: (1) Two starburst events describing discontinuous star formation due to episodic fueling with molecular gas and (2) continuous star formation assuming continuous fueling with molecular gas and/or a large nuclear reservoir of gas.

In a first step we tried to fit the diagnostic ratios for the two different scenarios. When the predicted L_K and L_{LyC} luminosities were matched to the observed values. The spectral synthesis was used to address the non-stellar properties of the nuclear region such as extinction, dust emission or AGN continuum contribution which also effect the overall values. However, the derived values are rather small: For the spectral synthesis fitting (which is independent of L_K , since it is tied to the calibrated spectrum), we tried apparent extinction values of $A_V=1^{mag}$, 2^{mag} , 3^{mag} , 4^{mag} and 5^{mag} . For the two star formation scenarios considered here, we find an extinction of $(2 - 3)^{mag}$ (mainly affecting the slope of the K band spectrum at shorter wavelength end) combined with a $\sim 5\%$ non-stellar contribution to the K band continuum which is either due to emission from warm dust ($T \sim 500$ K) or AGN power law emission (affecting the slope of the K band spectrum at the longer wavelength end). We used the mean flux density at large radii ($r \sim 3.5''$) to estimate the contribution of the underlying old bulge population to about 10 % of the K band continuum flux density in a $3''$ aperture. However, the bulge population has a much larger spatial extent than the stellar cluster mapped in its stellar absorption lines.

Both star formation possibilities are explored in the following. The model parameters and results of the star forming events for the different scenarios are given in Tab. 3.

5.3.1. Two Young Starburst Events

As discussed in section 5.2 the WR stars have an age of about 3 - 5 Myr. This low age immediately implies a second starburst or star formation event that is responsible for the cool evolved stars indicated by the stellar absorption features (s. section 4.3).

Starburst about 3 - 5 Myr ago (SB#1): Assuming a starburst event with a decay time of 3 Myr seems reasonable given the fact that SN explosions might disturb the ISM and prevent further star formation. For a starburst in that age range, STARS gives a mean ionizing hot star of type O7 to O5 with a mean effective temperature of $T_{eff} \approx 40000 - 45000$ K. Neglecting dilution effects

(s. section 4.1) this corresponds to an HeI/Br γ ratio of 0.7 (Lançon & Rocca-Volmerage 1996). A comparison of K band spectra from galaxies with AGN and pure starburst galaxies (Vanzi et al. 1998) suggests that a strong HeI emission line is only present in the pure starburst galaxies without an AGN. This probably indicates that most of the HeI line flux observed towards the nucleus of NGC 6764 is due to young, hot stars and not due to an AGN component. Under the assumption that all HeI line flux is associated with the starburst, we can correct the observed HeI/Br γ ratio of 0.46 ± 0.04 to obtain the Br γ line flux associated with the starburst event. To fit the model ratio of 0.7 about 65% of the observed Br γ line flux has to be due to the 5 Myr old starburst. This finding is in excellent agreement with the value of 66% for the H α line emission of Gonçalves, Veron-Cetty & Veron (1999). By fitting L_{LyC} , we obtained the contributions of this starburst to L_K , L_{bol} and ν_{SN} . The remaining differences in these quantities have to be attributed to the second starburst (or star formation) event and are used for the further model fits.

Starburst about 25 Myr ago (SB#2): The first starburst contributes only a few percent to the K band luminosity, and the old bulge population delivers about 10 % (see section 5.3). Therefore, this second starburst has to account for about 85% of the total L_K and the total amount of ν_{SN} without further large contributions to L_{LyC} . A ~ 15 Myr old starburst can account for most of the remaining L_{LyC} . However, if the age is about 25 Myr almost all of the remaining 35% of the Br γ line flux could be associated with the LINER nucleus (s. Table 3). At an age of 50 Myr, the contribution of this starburst to the Lyman continuum is already negligible and only small to the nuclear radio continuum. We also tested ages of ~ 1 Gyr where AGB stars have a prominent contribution to the K band continuum (Lançon 1999, Lançon et al. 1999). This possibility can be ruled out, since at that age the radio emission could no longer be explained by star formation, i.e. synchrotron emission from SN remnants. The age for this second starburst event can not be so strict as in the case of the WR starburst, since it is not possible to absolutely constrain the contribution of this starburst to the K band luminosity, the Lyman continuum luminosity and the SN rate. However, its age has to be larger than 15 Myr and below 50 Myr which is well below 1 Gyr. Also, an underlying low-level constant star formation is impossible, since such a population can not produce the L_K needed without large contributions to L_{LyC} (see section 5.3.2).

This scenario is quite opposite to the one found in IC 342 where a 70 pc diameter starburst ring with an age of about 5 Myr surrounds a nuclear starburst of about 15 Myr (Böker, Förster-Schreiber & Genzel 1997). In NGC 6764 the younger component (*SB#1*) is concentrated in the nucleus and surrounded or embedded in the older star formation event (*SB#2*). Higher angular resolution would allow us to investigate if the *SB#1* component is indeed concentrated on the nucleus or is distributed in a small ring like in IC 342. A comparison of the contribution of the two starburst events to the optical continuum shows that the WR burst contributes about 15% to the synthesized stellar V band continuum. This is in agreement with the 11% continuum contribution derived by Osterbrock & Cohen (1982).

5.3.2. Continuous Star Formation

If we assume continuous star formation in the nuclear region the nuclear stellar population must have an age of ≥ 1 Gyr, since only then enough cool evolved stars have been produced to obtain the observed ratio of L_K to L_{LyC} . It is necessary to reach at least the AGB phase for a reasonable fit, since only then enough of the observed cool luminous stars are present. This analysis is, however, hampered by the fact, that the evolutionary tracks of the high mass stars do not produce very cold red supergiants (e.g. of type M) and that SPECSYN does not use spectra of AGB stars. The spectra of AGB stars are approximated by those of a red supergiant (RSG) of type M4Iab. This may affect the slope at the beginning of the K band, however, SPECSYN spectra start only at $2.0267 \mu\text{m}$ there this effect is already weak. Since only a small fraction of the total K band light is due to AGB stars, this is negligible and for the purpose of the NIR spectral synthesis sufficient. The derived star formation rate (SFR) of this scenario is $\sim 0.3 M_\odot/\text{yr}$. For an age of the stellar population of 1 Gyr this translates into about $3 \times 10^8 M_\odot$ of molecular gas that have been transformed into stars. The average star formation efficiency (SFE) in giant molecular cloud complexes (GMCs) is of the order of a few percent (Duerr et al. 1982, Tenorio-Tagle & Bodenheimer 1988), up to values of 30 - 40 % only in the densest cores of these complexes (Lada 1982; see summary article by Lada, Strom & Myers 1993). If we assume an average value of up to 10% for molecular clouds in starburst environments, the mass inflow rate needed is about 3 - 6 M_\odot/yr . Bars are relative efficient in transporting gas down to small radii, Jogee, Kenney & Smith (1999) found a mass inflow rate of about 1 M_\odot/yr for the central starburst in NGC 2782. However, Eckart et al. (1991) estimated a total molecular gas mass of 2 - 6 $\times 10^8 M_\odot$ for NGC 6764. Together with the fact that bars are short-lived features in the evolution of galaxy ($\sim 10^8$ yrs; Combes 1998), such a high inflow rate over 1 Gyr seems highly unlikely.

Another aspect of this scenario is that the WR emission (HeI and Br γ line) and the stellar absorption bands should have similar distributions even at highest spatial resolution. However, this is already in contradiction to the observed spatial distribution of the H and He recombination lines (unresolved) versus the extent of the stellar absorption lines (similar to K band continuum). It might be a possible scenario that due to dispersion of the nuclear stellar cluster the older stars have moved to larger radii. A comparison to the upper limit of $\sim 3 \times 10^9 M_\odot$ for the total mass in the inner 5" (Eckart et al. 1991) shows that the converted gas mass is only a small fraction ($\sim 10\%$) and therefore we expect the gravitational potential to minimize such an effect. In addition, a continuous star formation would account for the total H recombination line emission without any emission arising from the AGN. Therefore continuous star formation is highly unlikely, although the spectral fit (see Fig. 6) is equally satisfying.

6. SUMMARY AND CONCLUSIONS

NGC6764 shows strong variations in its X-ray flux density by at least a factor of 2 on time-scales of 7 days. This suggests the presence of a compact AGN with an upper size estimate of

$R \approx \Delta t c \approx 1.6 \times 10^{16}$ cm or only about 10^3 AU. In addition there is evidence for an extended and possibly soft diffuse component of the X-ray emission. The hot X-ray emitting gas and the synchrotron radiation emitting relativistic gas component are spatially coexisting and are probably both the result of strong recent nuclear star formation.

NIR integral field spectroscopy of the nuclear region in the WR LINER galaxy NGC 6764 reveals that the nuclear star formation is probably confined to two areas, one of less than 100 pc (WR stars) and the other with an extent of ~ 200 pc (RSGs): The WR stars and the evolved cool stars are not co-spatial and the younger starburst resides inside the older starburst. This picture is quite contrary to what is observed in many starburst galaxies where the younger component is arranged in a ring around the older nucleus (e.g. NGC 7552: Schinnerer et al. 1997, IC 342: Böker, Förster-Schreiber & Genzel 1997).

Application of a population synthesis in conjunction with NIR spectral synthesis infers an extinction towards the nuclear stellar cluster of about $(2 - 3)^{mag}$ in agreement with the observed $Br\delta/Br\gamma$ ratio and earlier findings by Eckart et al. (1996). In addition we see evidence for a 5% non-stellar contribution to the K band continuum either from warm dust or a power law contribution from the AGN itself. In a $3''$ aperture the K band contribution of the bulge population is about 10%.

The nuclear star formation history allows for two simple possibilities: (1) Two starbursts with ages of 3 to 5 Myr and between 15 and < 50 Myr and decay times of 3 Myr which produce the WR stars and red supergiants that contribute to a large amount of the K band continuum. (2) Continuous star formation with a SFR of $\sim 0.3 M_{\odot}/yr$ for at least 1 Gyr.

In the case of the 'two starburst' scenario, an analysis of the H and He recombination lines shows that about 65% of the $Br\gamma$ line emission is associated with the young starburst, leaving the rest for the LINER nucleus or/and the second starburst event. Comparison of our data and data from the literature with population synthesis results for WR dominated cluster suggests an age of 3 - 5 Myr for the WR component in NGC 6764. The age for the second starburst event is in the range of 15 Myr to well below 1 Gyr depending on the contribution of this starburst to the Lyman continuum and the radio continuum observed.

The continuous star formation scenario seems highly unlikely given the larger amount of molecular gas needed to be transported down to radii of ~ 160 pc over 1 Gyr. In addition, the spatial distribution of the line emission is expected to be cospatial with the stellar absorption lines - this is not observed. Even if we allowed for an unresolved 35% AGN contribution to the $Br\gamma$ such a case seems unlikely, because there is no indication for extended emission on a lower level in the radial profile of the $Br\gamma$ line emission. Therefore, the most likely scenario is that two recent starbursts have occurred in the nuclear region of NGC 6764.

The nucleus of NGC 6764 exhibits an interesting star formation scenario, since the younger component seems more compact than the older one. One explanation could be that the bar is transporting the molecular gas very close to the nucleus (< 50 pc). In that case the star formation might directly compete with the AGN for the fuel. It may also influence or even control the AGN activity. The presence of a compact AGN (from the X-ray data) and violent recent nuclear star formation underline the composite nature of the nucleus of NGC 6764.

We like to thank the MPE 3D group, especially N. Thatte, J.F. Gallimore, M. Tecza and N.M. Förster-Schreiber, for their help taking the data. We also thank the Calar Alto 3.5 m telescope staff for hospitality and support. We are grateful to A. Sternberg for providing us with the population synthesis code STARS. We also want to thank the anonymous referee for her/his valuable comments which helped to improve the paper.

References

- Armus, L., Heckman, T.M., Miley, G.K., 1988, *Ap. J. (Letters)*, 326, L45.
- Baum, S.A., O’Dea, C.P., Dallacassa, D., de Bruyn, A.G., Pedlar, A., 1993, *Ap. J.*, 419, 553.
- Böker, T., Förster-Schreiber, N.M., Genzel, R., 1997, *A. J.*, 114, 1883.
- Boer, B., Schulz, H., 1989, in ‘Extranuclear Activity in Galaxies’, ESO Workshop, held in Garching, F.R.G., May 16-18, 1989, ed. E.J.A. Meurs and R.A.E. Fosbury; Publisher, European Southern Observatory, Garching bei München, p. 299
- Condon, J. J., 1992, *Ann. Rev. Astron. Astrophys.*, 30, 575.
- Boller, Th., 1999, *Ap. & S.S.*, 266, 49
- Conti, P.S., 1991, *Ap. J.*, 377, 115.
- David, L.P., Harnden, F.R., Kearns, K.E., Zombeck, M.V., 1996, *The ROSAT High Resolution Imager*. SAO Press, Cambridge
- Dickey, J.M., Lockman, F.J., 1990, *ARAA*, 28, 215
- Doherty, R.M., Puxley, P.J., Lumsden, S.L., doyon, R., 1995, *M.N.R.A.S.*, 277, 577.
- Doyon, R., Joseph, R.D., Wright, G.S., 1994, *Ap. J.*, 421, 101.
- Duerr, R., Imhoff, C.L., Lada, C.J., 1982, *Ap. J.*, 261, 135.
- Eckart, A., Cameron, M., Boller, Th., Krabbe, A., Blietz, M., Nakai, N., Wagner, S.J., Sternberg, A., 1996, *Ap. J.*, 472, 588.
- Eckart, A., Cameron, M., Jackson, J.M., Genzel, R., Harris, A.I., Wild, W., Zinnecker, H., 1990, *Ap. J.*, 372, 67.
- Figer, D.F., McLean, I.S., Najarro, F., 1997, *Ap. J.*, 486, 420.
- Förster-Schreiber, N.M., 2000, *A.J.*, accepted
- Gehrz, R.D., Sramek, R.A., and Weedman, D.W., 1983, *Ap. J.*, 267, 551.
- Genzel, R., Weitzel, L., Tacconi-Garman, Blietz, M., Krabbe, A., Lutz, D., Sternberg, A., 1995, *Ap. J.*, 444, 129.
- Gonçalves, A.C., Veron-Cetty, M.-P. & Veron, P., 1999, *Astron. Astrophys. Suppl.*, 135, 437.
- Jogee, S., Kenney, J.D.P., Smith, B.J., 1999, *Ap. J.*, 526, 665.
- Kleinmann, S.G., Hall, D.N.B., 1986, *Ap. J. Supp.*, 62, 501.
- Krabbe, A., Sternberg, A., and Genzel, R., 1994, *Ap. J.*, 425, 72.

- Kriss, G.A., Canizares, C.R., Ricker, G.R., 1980, *Ap. J.*, 242, 492.
- Kunth, D., Contini, T., 1999, in 'Wolf-Rayet Phenomena in Massive Stars and Starburst Galaxies', Proc. IAU Symposium 193, ed. K.A. van der Hucht, G. Koenigsberger & P.R.J. Eenens, p. 725
- Lada, E.A., 1992, *Ap. J. (Letters)*, 393, L28.
- Lada, E.A., Strom, K.M., Myers, P.C., 1993, in "Protostars and Planets III", p. 245
- Lançon, A., 1999, 'Asymptotic Giant Branch Stars', IAU Symposium 191, in press, astro-ph9810474
- Lançon, A., Mouhcine, M., Fioc, M., Silva, D., 1999, *Astron. Astrophys.*, 344, L21.
- Lançon, A., Rocca-Volmerange, B., 1996, *New. A.*, 1, 215
- Larson, R. B., Tinsley, B. M., 1978, *Ap. J.*, 219, 46.
- Leitherer, C. et al., 1999, *Ap. J. Supp.*, 123, 3.
- Leitherer, C., Heckman, T.M., 1995, *Ap. J. Supp.*, 96, 9.
- Lord, S., 1992, NASA Technical Memorandum 103957, Ames Research Center, Moffett Field, CA
- Maeder, A., Conti, P.S., 1994, *ARAA*, 32, 227
- Maiolino, R., Krabbe, A., Thatte, N., Genzel, R., 1998, *Ap. J.*, 493, 650.
- Mas Hesse, J.M., and Kunth, D., 1991, *Astr.Ap.Suppl.* 88, 399
- Meynet, G., Maeder, A., Schaller, G., Schaerer, D., Charbonnel, C., 1994, *Astron. Astrophys. Suppl.*, 103, 97.
- Oliva, E., Origlia, L., 1998, *Astron. Astrophys.*, 332, 46.
- Oliva, E., Origlia, L., Kotilainen, J.K., Moorwood, A.F.M., 1995, *Astron. Astrophys.*, 301, 55.
- Origlia, L., Moorwood, A.F.M., Oliva, E., 1993, *Astron. Astrophys.*, 280, 536.
- Origlia, L., Oliva, E., 2000, *Astron. Astrophys.*, 357, 61.
- Osterbrock, D.E., 1989, *Astrophysics of Gaseous Nebulae and Galactic Nuclei*, University Science Books, Mill Valley, California
- Osterbrock, D.E., Cohen, R.D., 1982, *Ap. J.*, 261, 64.
- Raymond, J.C., Smith, B.W., 1977, *ApJS*35419
- Rieke, G.H., 1978, *Ap. J.*, 226, 550.
- Rieke, G. H., Lebofsky, M. J., Thompson, R. I., Low, F. J., Tokunaga, A. T., 1980, *Ap. J.*, 238, 24.
- Rieke, G. H., Loken, K., Rieke, M. J., Tamblyn, P., 1993, *Ap. J.*, 412, 99.

- Rubin, V.C., Thonnard, N., Ford, W.K., 1975, *Ap. J.*, 199, 31.
- Sanders, D.B., Mirabel, I.F., 1996, *Ann. Rev. Astron. Astrophys.*, 34, 749.
- Schaerer, D., Charbonnel, C., Meynet, G., Maeder, A. Schaller, G., 1993, *Astron. Astrophys. Suppl.*, 102, 339.
- Schaerer, D., Contini, T., Pindao, M., 1999, *Astron. Astrophys. Suppl.*, 136, 35.
- Schaerer, D., Vacca, W.D., 1998, *Ap. J.*, 497, 618.
- Schinnerer, E., Eckart, A., Quirrenbach, A., Böker, T., Tacconi-Garman, L.E., Krabbe, A., Sternberg, A., 1997, *Ap. J.*, 488, 174.
- Schinnerer, E., Eckart, A., Tacconi, L.J., 1998, *Ap. J.*, 500, 147.
- Schinnerer, E., Eckart, A., Tacconi, L.J. et al., 2000, in prep.
- Schmidt, M., Green, R.F., 1986, *Ap. J.*, 305, 68.
- Telesco, C.M., Dressel, L.L., Wolstencroft, R.D., 1993, *Ap. J.*, 414, 120.
- Tenorio-Tagle, G., Bodenheimer, P., 1988, *ARA&A*26145
- Thatte, N.A., Kroker, H., Weitzel, L., Tacconi-Garman, L.E., Tecza, M., Krabbe, A., Genzel, R., 1995, *Proc. SPIE Vol. 2475*, 228
- Trümper, J., 1983, *Adv. Space Res.*, 4, 241
- Ulvestad, J.S., Wilson, A.S., Sramek, R.A., 1981, *Ap. J.*, 247, 419.
- Vanzi, L., Alonso-Herrero, A., Rieke, G.H., 1998, *Ap. J.*, 504, 93.
- Walter R., Fink H., 1993, *Astron. Astrophys.*, 274, 105.
- Weitzel, L., Krabbe, A., Kroker, H., Thatte, N., Tacconi-Garman, L. E., Cameron, M., Genzel, R., 1996, *Astron. Astrophys. Suppl.*, 119, 531.
- Wilson, A.S., Willis, A.G., 1980, *Ap. J.*, 240, 429.

Table 1: Emission line fluxes in NGC 6764

| Aperture ["] | Br δ 1.945 μm | He I 2.058 μm | Br γ 2.166 μm | Br δ /Br γ | He I/Br γ |
|-----------------|------------------------------------|-----------------------------|------------------------------------|--------------------------|------------------|
| 2.00 | 3.37 ± 0.48 | 2.14 ± 0.16 | 4.64 ± 0.20 | 0.73 ± 0.11 | 0.46 ± 0.04 |
| 3.00 | 3.90 ± 0.72 | 2.93 ± 0.24 | 6.40 ± 0.29 | 0.61 ± 0.12 | 0.46 ± 0.04 |
| 4.00 | 4.95 ± 0.94 | 3.00 ± 0.31 | 7.59 ± 0.38 | 0.65 ± 0.13 | 0.39 ± 0.05 |
| 5.00 | 5.71 ± 1.21 | 3.30 ± 0.40 | 8.20 ± 0.49 | 0.70 ± 0.15 | 0.40 ± 0.05 |

Emission line fluxes are given in units of $10^{-18} \text{ W m}^{-2} = 10^{-15} \text{ ergs cm}^{-2} \text{ s}^{-1}$. The given errors are the standard deviations (1σ). The lines were measured in the combined data with an angular resolution of $\sim 1.2''$.

Table 2: Absorption line equivalent widths in NGC 6764

| Aperture ["] | Na I 2.206/2.209 μm | $^{12}\text{CO}(2-0)$ 2.294 μm | $^{12}\text{CO}(3-1)$ 2.323 μm | $^{13}\text{CO}(2-0)$ 2.345 μm |
|-----------------|-----------------------------------|--|--|--|
| 2.00 | 2.81 ± 0.71 | 13.29 ± 1.46 | 14.52 ± 2.58 | 8.61 ± 3.53 |
| 3.00 | 2.86 ± 0.68 | 13.09 ± 1.40 | 13.72 ± 2.48 | 10.06 ± 3.39 |
| 4.00 | 2.70 ± 0.70 | 13.70 ± 1.47 | 14.61 ± 2.60 | 11.04 ± 3.55 |
| 5.00 | 1.66 ± 0.75 | 14.06 ± 1.61 | 13.64 ± 2.85 | 11.54 ± 3.90 |

Absorption line equivalent widths given in \AA . The given errors are the standard deviations (1σ). The lines were measured in the combined data with an angular resolution of $\sim 1.2''$. We used the definitions for the absorptions lines as given in Origlia et al. 1993.

Table 3: Star Formation Scenarios in the Nucleus

| | Obs. | SB #1 ^a | SB #1 ^b | SB #2 ^c | SB #2 ^d | SB #2 ^e | Cont. |
|--|------|--------------------|--------------------|--------------------|--------------------|--------------------|-------|
| L_K [$10^7 L_\odot$] | 9.9 | 0.2 | 0.3 | 8.4 | 8.4 | 8.4 | 9.9 |
| L_{LyC} [$10^8 L_\odot$] | 3.9 | 2.6 | 2.6 | 1.4 | 0.2 | 0.0 | 4.1 |
| L_{bol} [$10^9 L_\odot$] | 9.0 | 1.3 | 2.1 | 6.3 | 7.5 | 5.4 | 6.3 |
| ν_{SN} [10^{-2} yr^{-1}] | 1.2 | 0.0 | 0.1 | 1.4 | 3.0 | 0.1 | 0.5 |
| m_{st} [$10^7 M_\odot$] | | 0.1 | 0.1 | 1.7 | 4.5 | 8.0 | 12.0 |
| m_{gas} [$10^7 M_\odot$] | | 0.1 | 0.1 | 2.2 | 6.5 | 13.1 | 29.2 |

The observed values are derived assuming $A_V=2^{mag}$ and using the following measured values in a 3" aperture: $S_K=6.74\text{mJy}$, $S_{5GHz}=3.4\text{mJy}$, $F_{Br\gamma}=64.0\times 10^{-16}$ ergs cm^{-2} . The equations can be found in Schinnerer, Eckart & Tacconi (1998). m_{st} and m_{gas} denote the present-day stellar mass and the consumed gas mass to date, respectively.

All starburst models are calculated using a Salpeter IMF with mass cut-offs of $1 M_\odot$ to $120 M_\odot$.

SB #1^a: age of 3 Myr and decay time of 3 Myr (WR stars).

SB #1^b: age of 5 Myr and decay time of 3 Myr (WR stars).

SB #2^c: age of 15 Myr and decay time of 3 Myr (RSGs).

SB #2^d: age of 25 Myr and decay time of 3 Myr (RSGs).

SB #2^e: age of 50 Myr and decay time of 3 Myr (RSGs).

Cont. : age ≥ 1 Gyr and continuous star formation.

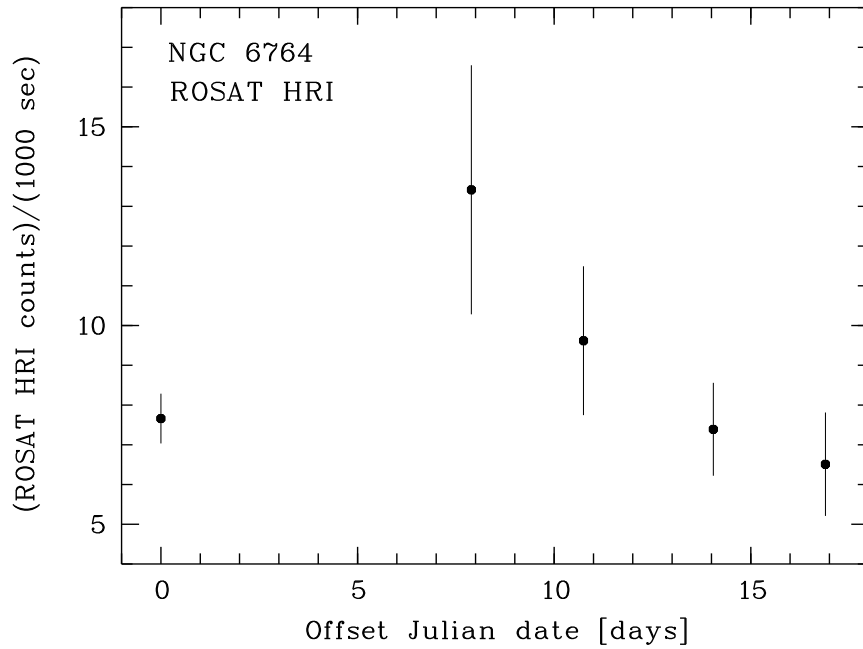


Fig. 1.— ROSAT HRI light curve of NGC 6764. The abscissa label gives the offset Julian date. Each data point is plotted in the middle of the exposure interval from which it was obtained, and the sizes of the exposure intervals lie within the data points themselves. NGC 6764 shows indications for count rate variations by a factor of about 2 within a few days (see text for details).

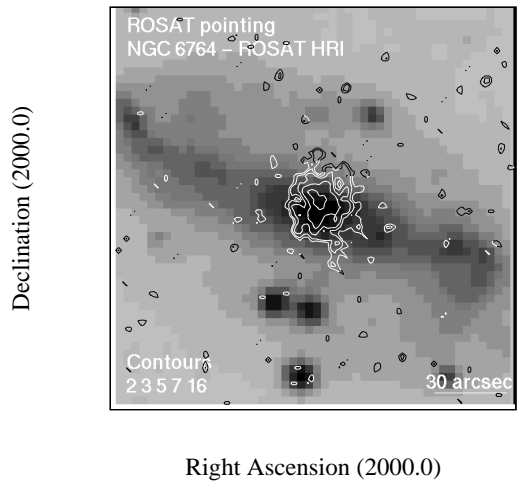


Fig. 2.— Pointed ROSAT HRI image of NGC 6764 in contours overlaid on an optical Digitized Sky Survey grayscale image. The X-ray emission is clearly extended in north-south direction.

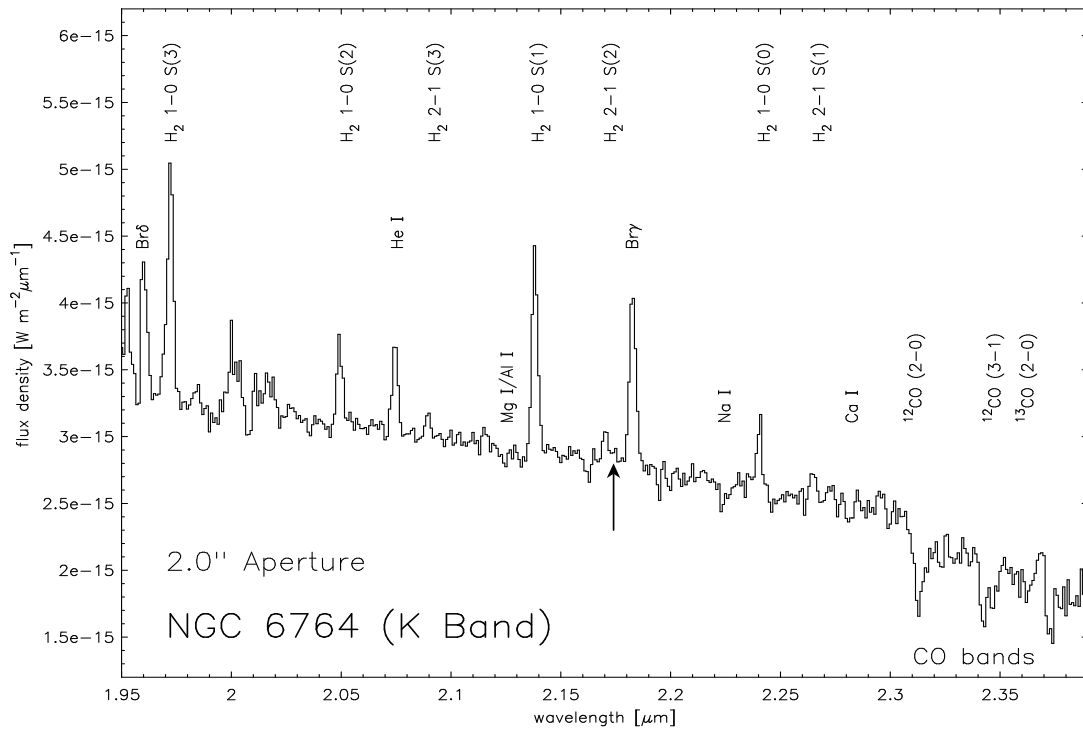


Fig. 3.— *K* band spectrum of the inner 3'' of NGC 6764. The detected lines are indicated. The arrow marks the position of the HeI/HeII line complex discussed in section 5.2 (see also Fig. 5).

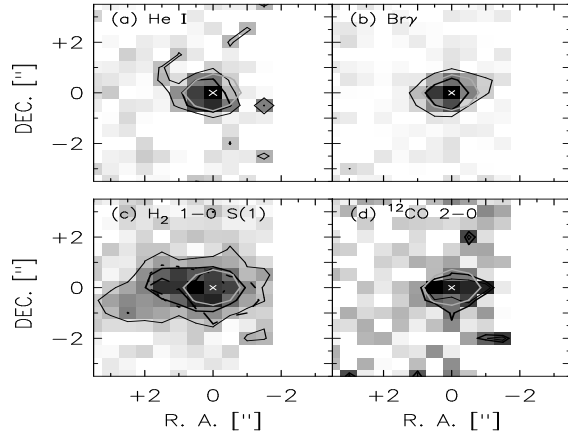


Fig. 4.— Maps of the (a) HeI, (b) Br γ and (c) H₂1-0 S(1) line emission as well as the (d) ¹²CO (2-0) absorption line from the July 26 data cube. The 50% contours of the lines (fat black line) and the adjacent continuum (fat grey line) are indicated as well as the 2 σ contour (thin black line). The blue (dashed contour) and red (dotted contour) wing of the H₂1-0 S(1) line emission are given as well.

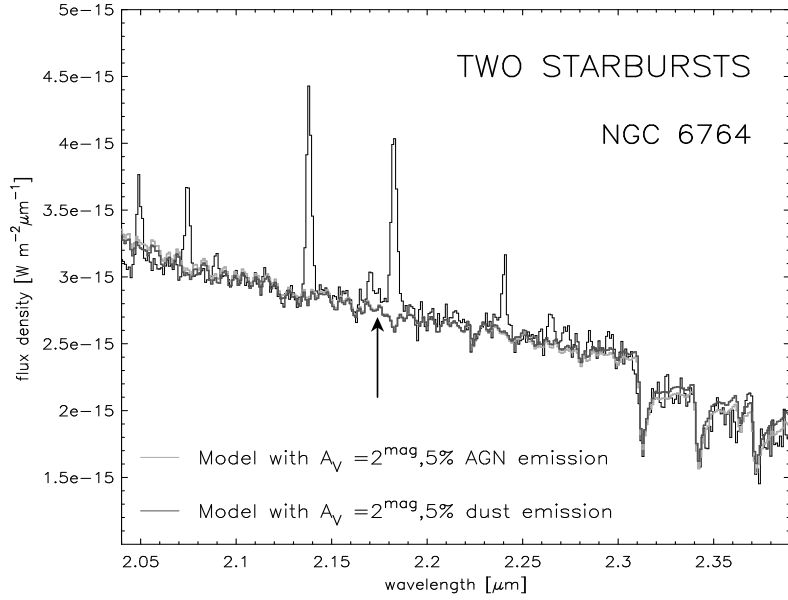


Fig. 5.— Comparison of the observed spectrum to the synthesized spectrum for the case of the two starbursts. We used ages for the two starburst events of 5 Myr and 25 Myr (see also Table 3). The arrow marks the position of the HeI/HeII line complex discussed in section 5.2.

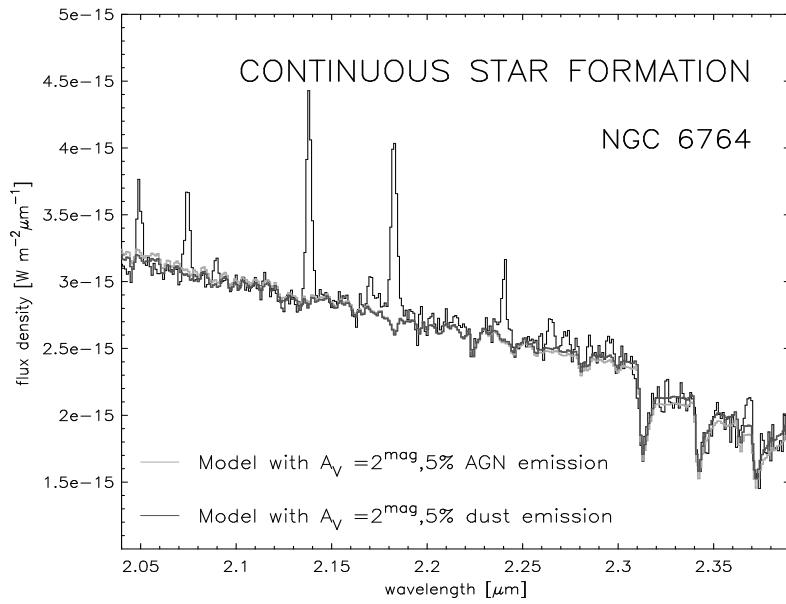


Fig. 6.— Comparison of the observed spectrum to the synthesized spectrum for the case of the continuous star formation.